



Article

Impact of Land Use/Land Cover Change on Ecological Quality during Urbanization in the Lower Yellow River Basin: A Case Study of Jinan City

Guangting Yu ^{1,2,3}, Tongwen Liu ^{1,2,3}, Qi Wang ^{1,2,3,*}, Tao Li ^{1,2,3}, Xiuqing Li ^{1,4}, Guanhan Song ^{1,2,3} and Yougui Feng ^{1,5}

¹ School of Surveying and Geo-Informatics, Shandong Jianzhu University, Jinan 250101, China

² Shandong Institute of Geological Surveying and Mapping, Jinan 250013, China

³ Geological Big Data Development and Application Engineering Technology Research Center, Shandong Provincial Bureau of Geology and Mineral Resources, Jinan 250013, China

⁴ School of Geography and Environment, Shandong Normal University, Jinan 250358, China

⁵ Shandong Zhengyuan Aerial Remote Sensing Technology Co., Ltd., Jinan 250101, China

* Correspondence: wangqi19@sdjzu.edu.cn



Citation: Yu, G.; Liu, T.; Wang, Q.; Li, T.; Li, X.; Song, G.; Feng, Y. Impact of Land Use/Land Cover Change on Ecological Quality during Urbanization in the Lower Yellow River Basin: A Case Study of Jinan City. *Remote Sens.* **2022**, *14*, 6273. <https://doi.org/10.3390/rs14246273>

Academic Editor: Stuart Phinn

Received: 8 October 2022

Accepted: 8 December 2022

Published: 11 December 2022

Publisher's Note: MDPI stays neutral with regard to jurisdictional claims in published maps and institutional affiliations.



Copyright: © 2022 by the authors. Licensee MDPI, Basel, Switzerland. This article is an open access article distributed under the terms and conditions of the Creative Commons Attribution (CC BY) license (<https://creativecommons.org/licenses/by/4.0/>).

Abstract: Rapid urbanization in the lower Yellow River basin has greatly contributed to the socio-economic development of Northern China, but it has also exacerbated land use/land cover change, with significant impacts on ecology. Ecological quality is a comprehensive spatial and temporal measure of an ecosystem's elements, structure and function, reflecting the ecological state under external pressures. However, how land use/land cover change affects the ecological quality during urbanization has rarely been explored. In this study, Jinan, a megacity in the lower Yellow River basin, was taken as a typical region, and the response of ecological quality to the land use/land cover change in 2000, 2010 and 2020 was retrieved using the remote sensing ecological index. For the mixed land use/land cover change types, a type-decomposition and spatial heterogeneity quantification method based on the abundance index was proposed, and the impact mechanisms of the land use/land cover change on the ecological quality were revealed by coupling with GeoDetector. The results show that: (1) Farmland and built-up areas, as the dominant land use/land cover types, were the primary factors controlling the spatial pattern of ecological quality. (2) Urban expansion and farmland protection policies resulted in the transfer of farmland and woodland to built-up areas as well as the transfer of woodland and grassland to farmland, which intensified the degradation of ecological quality. (3) Ecological protection policies prompted the transfer of farmland and grassland to woodland and the transfer of farmland to grassland as the main cause for the improvement of ecological quality. (4) Although ecological protection and urban development were implemented in parallel, uneven land use/land cover changes resulted in a 1.4 times expanded area of poorer ecological quality with increasingly serious spatial agglomeration effects. This study can provide scientific references for the ecological conservation and high-quality, sustainable development of cities in the lower Yellow River basin.

Keywords: land use/land cover change; remote sensing ecological index; ecological quality; GeoDetector; Jinan City; Yellow River basin

1. Introduction

Rapid urbanization has brought about economic changes and dramatic changes in land cover from natural landscapes to built-up areas due to increasing human activities [1,2]. This has led to a series of negative ecological effects [3], including land degradation [4], urban heat island [5], droughts [6], flash floods [7], biodiversity reduction [1], ecosystem cycle destruction [8] and ecosystem service decline [9], which have had significant impacts and pressures on ecology [10]. The relationship between urbanization and ecology is a

complex interaction and coupling process [2]. Ecological quality is a comprehensive spatial and temporal measure of an ecosystem's elements, structure and function, reflecting the ecological state under external pressures and the suitability for human survival and sustainable socio-economic development [11,12]. Therefore, carrying out dynamic monitoring and evaluation of ecological quality is crucial to reveal the trigger mechanism of ecological degradation in the context of urbanization, which will provide an important basis for the realization of sustainable development goals [13] and the formulation of ecological environmental protection policies.

As an important ecological function region in China [14], the Yellow River basin (YRB) is also one of the most ecologically fragile regions in China [13]. In recent decades, urbanization has formed an impressive economic development belt and urban agglomeration in the YRB [15]. However, in the process of urbanization, the YRB has also experienced long-term disordered development and land use, resulting in many ecological and environmental problems [16]. In particular, the downstream area, which has the highest level of economic development in the YRB, has a high urban density, a large population and a high intensity of land exploitation, and the urbanization level is now higher than 60% [6,17]. Its rapid urbanization has greatly contributed to the socio-economic development of Northern China but has also greatly exacerbated the land use/land cover change (LUCC), which has particularly significant impacts on ecology [17,18]. Therefore, monitoring and evaluating the quality of urban ecology in the context of urbanization and exploring the relationship between urban development and ecological impacts in this region are essential for future planning, management, conservation and high-quality development [16].

With the development of remote sensing theory and application in recent years, many remote sensing parameters or indexes have been applied to ecological quality evaluation, such as net primary productivity (NPP), the normalized difference vegetation index (NDVI), land surface temperature (LST) [4,19,20], etc. However, ecological quality is the result of the combined effect of regional pressure–state–response (PSR) frameworks. Therefore, the single parameters or indexes above are not sufficient to reflect the state of regional comprehensive ecological quality and its changes [6]. In 2006, the Chinese Ministry of Environmental Protection designed a comprehensive ecological evaluation index (EI) [21,22]. This index integrates biological abundance, vegetation cover, water network density, land degradation and environmental quality, reflecting the comprehensiveness, completeness and hierarchy of ecological evaluation and is the most widely used standard by the Chinese government [13]. However, the problems of difficult access to land degradation and environmental indicators, difficult visualization and long data update cycles still limited its practical application [3,13]. To address this issue, Xu [23] proposed a remote sensing ecological index (RSEI) based on the PSR framework, which integrated greenness, wetness, dryness and heat indicators and could be completely based on the same remote sensing data. The basic indicators in RSEI are synthesized by principal component analysis (PCA), which can avoid differences and errors in the subjective weighting of indicators and is spatio-temporally scalable, visible and comparable [24]. Compared to EI, RSEI can also characterize the regional ecological quality well in an integrated manner [8] and is simpler to apply and easier to update [4].

The proposal of RSEI has extended the application of remote sensing in the assessment of the ecological status of the land surface [25]. Furthermore, RSEI has been widely used in recent years for rapid ecological quality evaluation on different scales, such as national and provincial regions [26–28], urban agglomerations [2,29,30], cities [11,19,31], drainage basins [6,32,33], lakes [3,34], islands [35,36], mining areas [37], protected areas [38], etc. In addition, many scholars have also used RSEI to analyze the relationship between changes in ecological quality and factors, such as urbanization [31], economic and industrial development [39], land consolidation [40], population and impervious surfaces [28,41], ecosystem services [12], natural climate change [42], landscape [43] and geological hazards [44], revealing the drivers of ecological quality change. Many studies have shown that land use and ecological composition are the main factors influencing the changes in ecological

quality [3,19,25]. In particular, the regional land use/land cover (LULC) structure has an important influence on the stability of the ecosystem structure and function [22] and dominates changes in ecological quality [2,24]. However, there are currently few studies on how regional LUCC affects the ecological quality changes.

To address the aforementioned issues, this study took Jinan, a megacity in the lower reaches of the YRB, as a typical region, to study the impact of urban LUCC on the ecological quality in the context of rapid urbanization and explore its driving mechanisms based on Landsat image data in 2000, 2010 and 2020. The main objectives of this study are to address the following questions: (1) How has LULC in Jinan changed from 2000 to 2020? (2) What are the spatio-temporal responses of ecological quality to LUCC? (3) How does LUCC drive changes in ecological quality, and how does it relate to land requirements and policies? The results of this study can provide scientific references for the ecological conservation and high-quality, sustainable development of cities in the lower YRB.

2. Materials and Methods

2.1. Study Area

Jinan City is located in the central part of Shandong Province, China (Figure 1a,b) and covers an area of 10,244 km². Jinan is bound by Mount Tai to the south and the Yellow River to the north. It is at the intersection of the low hills in central-southern Shandong and the alluvial plain in north-western Shandong, and the topography is high in the south and low in the north (Figure 1c). Jinan has a warm temperate continental monsoon climate with four distinct seasons, an average annual temperature of 13.6 °C and an average annual precipitation of 614.0 mm.

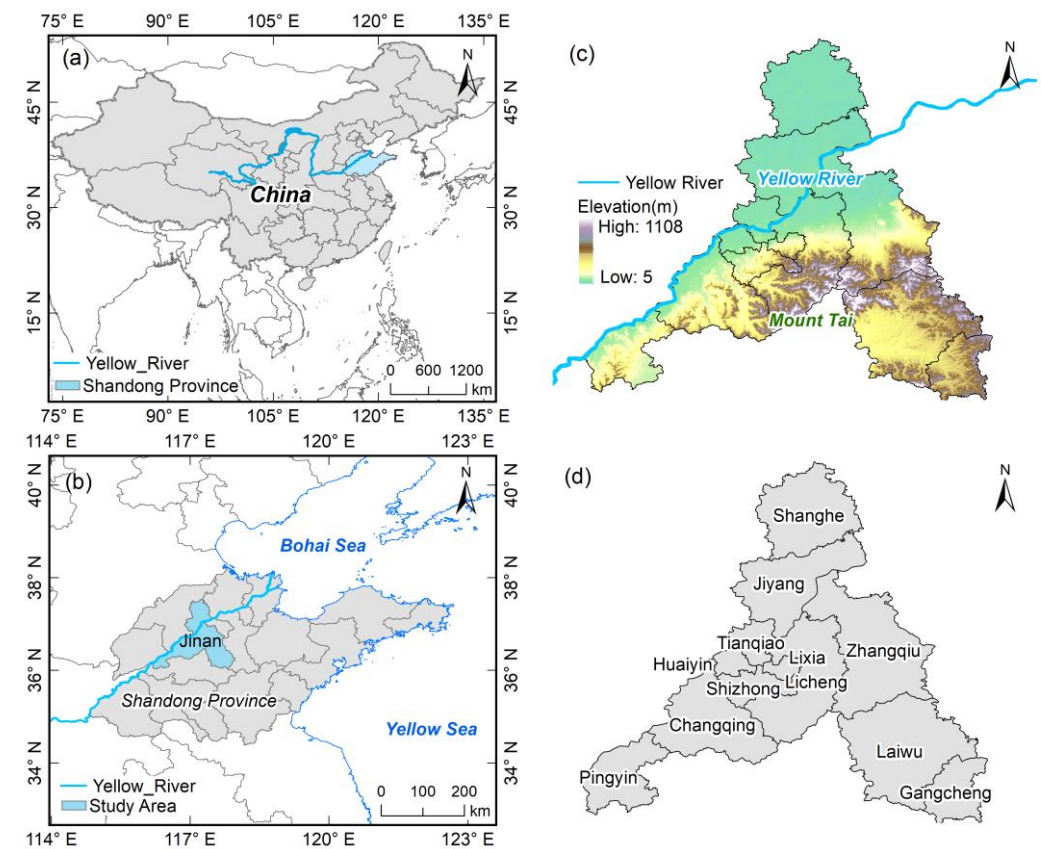


Figure 1. Overview of the study area: (a) location of the Shandong Province in China; (b) location of the study area in Shandong Province; (c) topography of the study area; (d) administrative division of the study area.

Jinan City is the political, economic, cultural, scientific, technological and educational center of Shandong Province, containing ten districts and two counties (Figure 1d). Jinan is at the intersection of many important development regions in China, with a prominent strategic position and unique geographical location. In addition, as a megacity in the lower YRB, Jinan is a typical representative of ecological protection and a core growth pole of high-quality development in the YRB.

Jinan has urbanized very rapidly in recent years. The information released by Jinan Municipal Government (<http://www.jinan.gov.cn/col/col129/index.html> (accessed on 19 August 2022)) shows that Jinan has experienced rapid urban expansion and a significant increase in urbanization rate, with a built-up area of 760.6 km². The 2021 Statistical Yearbook (<http://jntj.jinan.gov.cn/col/col27523/index.html> (accessed on 19 August 2022)) released by the Jinan Bureau of Statistics shows that the GDP in 2020 was CNY 1014.091 billion, an increase of up to 66.24% from 2015. According to the data of the seventh national census (2020) (<http://www.stats.gov.cn/tjsj/pcsj/rkpc/7rp/zk/indexch.htm> (accessed on 19 August 2022)), the resident population of Jinan has reached 9,202,400. Like many rapidly urbanizing cities, Jinan is facing ecological and environmental problems brought about by urbanization.

2.2. Data

The datasets used in this study include Landsat images and land use/land cover data interpreted based on Landsat images.

Landsat images have been widely used in the monitoring and assessment of LUCC and ecological status, which can better meet the application requirements in terms of temporal and spatial resolution. Vegetation cover is the most important influence factor in ecological quality evaluation. Therefore, we tried to select the images from July to August in summer, when the vegetation growth condition is the best. However, considering the increased rainfall in summer, there is less high-quality available data with cloud cover less than 5%, so we extended the available data range from June to October in the process of data acquisition. As shown in Table 1, we acquired six Landsat images from the USGS (<https://glovis.usgs.gov/app> (accessed on 7 August 2022)) for the years 2000, 2010 and 2020, all with less than 5% cloud coverage. Then, we preprocessed the images with ENVI 5.3 software for radiometric calibration, atmospheric correction, mosaic and clipping.

Table 1. Parameter information of Landsat images.

Year	Sensor Types	Strip Number	Line Number	Date	Cloud Coverage
2000	Landsat7 ETM+	122	34	14 September 2000	0.49%
		122	35	14 September 2000	0.15%
2010	Landsat7 ETM+	122	34	28 October 2010	0.00%
		122	35	28 October 2010	0.01%
2020	Landsat8 OLI	122	34	28 August 2020	2.78%
		122	35	28 August 2020	3.90%

To analyze the LUCC caused by urbanization in the study area in the past 20 years, we conducted LULC interpretation using eCognition Developer 9.0 software based on the previously acquired images. A total of 497 samples were labeled in the study area. Most of the samples were obtained through visual interpretation, whereas a small number of samples in the southern mountainous area were obtained from field survey data and national geoinformation survey. The object-oriented classification method based on the random forest model was used to classify the LULC of study area into woodland (WL), grassland (GL), farmland (FL), water body (WB), unutilized land (UL) and built-up areas (BA). The accuracy evaluation results show that the overall accuracy was 86.7%, which met the application requirements of this study.

2.3. Methods

The methodology used in this study contains three parts. First, the spatio-temporal characteristics of LUCC in the study area were analyzed using transfer matrix and dynamic degree index. Then, the RSEI was constructed from four indicators of greenness, wetness, dryness and heat to evaluate the ecological quality of the study area and its changes. Finally, the response mechanism of ecological quality to LUCC in the study area was revealed using GeoDetector.

2.3.1. Analysis of LUCC

- LULC Transfer Matrix

The transfer matrix (Equation (1)) can be used to analyze the structure and orientation of the LUCC, thus showing in detail the interconversion relationships and structural change characteristics among the LULCs [45]:

$$S_{ij} = \begin{bmatrix} S_{11} & S_{12} & \cdots & S_{1n} \\ S_{21} & S_{22} & \cdots & S_{2n} \\ \cdots & \cdots & \cdots & \cdots \\ S_{n1} & S_{n2} & \cdots & S_{nn} \end{bmatrix} \quad (1)$$

where S denotes the area; n is the number of LULCs before and after the transfer; i, j ($i, j = 1, 2, \dots, n$) denote the LULCs before and after the transfer, respectively; and S_{ij} denotes the area of type i transferred to type j . Each row element in the matrix denotes the flow information of type i transferred to other types, and each column element denotes the source information of other types transferred to type j .

- Dynamic Degree of LUCC

The dynamic degree of LUCC (Equation (2)) can quantitatively reflect the scale and change rate of a certain LULC in a given period and facilitate the prediction of future trends [46]:

$$K = \frac{U_b - U_a}{U_a} \times \frac{1}{T} \times 100\% \quad (2)$$

where K is the dynamic degree of LULC; U_a and U_b are the areas at the beginning and end of the given period; T is the time span of the given period; and when the unit of T is year, K is the annual change rate of the area.

2.3.2. Ecological Quality Evaluation

RSEI is widely used to evaluate the ecological quality status. Firstly, the four indicators of greenness, humidity, dryness and heat, which can be intuitively perceived by humans, were obtained through remote sensing inversion, and then the four indicators were normalized and synthesized using principal component analysis [23]. Further, the first principal component is taken to assess the ecological quality status of the region, and if the eigenvalues of greenness and wetness, which have a positive impact on ecology, are negative, the calculated results need to be reduced (Equation (3)). To facilitate comparison, the results of the RSEI calculation are also usually normalized (Equation (4)), and the closer the value is to 1, the better the ecological quality is, and vice versa, the worse it is.

$$RSEI_0 = \begin{cases} PC1[f(G, W, T, D)], EV_G, EV_W > 0 \\ 1 - PC1[f(G, W, T, D)], EV_G, EV_W < 0 \end{cases} \quad (3)$$

$$RSEI_n = \frac{RSEI_0 - RSEI_{0_min}}{RSEI_{0_max} - RSEI_{0_min}} \quad (4)$$

where G denotes greenness, W denotes wetness, T denotes heat, D denotes dryness, and EV_G, EV_W are eigenvalues of the greenness and wetness.

- Greenness

Vegetation cover has a significant effect on regional ecological quality. The NDVI can visually reflect plant growth and density and is an important indicator of regional vegetation cover. Hence, NDVI (Equation (5)) is used to characterize the greenness:

$$NDVI = (\rho_{nir} - \rho_{red}) / (\rho_{nir} + \rho_{red}) \quad (5)$$

where ρ_{nir} denotes the near-infrared band, and ρ_{red} denotes the red band.

- Wetness

The wetness can reflect the water and heat balance of an area and, thus, has great reference value for ecological variability. The wetness index is extracted from the remote sensing images using tasseled cap transformation, which can better reflect the moisture of soil and plants. There are differences in the conversion formulas for different types of remote sensing images, and the specific formulas are as follows:

$$WET_{ETM} = 0.2626\rho_{blue} + 0.2141\rho_{green} + 0.0926\rho_{red} + 0.0656\rho_{nir} - 0.7629\rho_{swir1} - 0.5388\rho_{swir2} \quad (6)$$

$$WET_{OLI} = 0.1511\rho_{blue} + 0.1972\rho_{green} + 0.3283\rho_{red} + 0.3407\rho_{nir} - 0.7117\rho_{swir1} - 0.4559\rho_{swir2} \quad (7)$$

where ρ_{blue} denotes the blue band, ρ_{green} denotes the green band, ρ_{red} denotes the red band, ρ_{nir} denotes the near-infrared band, ρ_{swir1} denotes the short-infrared band 1, and ρ_{swir2} denotes the short-infrared band 2.

- Dryness

The land surface “dryness” is mainly reflected in buildings and bare soil in the regional environment. Therefore, the dryness indicator (normalized difference built-up and soil index, NDBSI) (Equation (8)) is synthesized from both the bare soil index (BSI) (Equation (9)) and the index-based built-up index (IBI) (Equation (10)):

$$NDBSI = (BSI + IBI) / 2 \quad (8)$$

$$BSI = \frac{[(\rho_{swir1} + \rho_{red}) - (\rho_{nir} + \rho_{blue})]}{[(\rho_{swir1} + \rho_{red}) + (\rho_{nir} + \rho_{blue})]} \quad (9)$$

$$IBI = \frac{\frac{2\rho_{swir1}}{\rho_{swir1} + \rho_{nir}} - \left[\frac{\rho_{nir}}{\rho_{nir} + \rho_{red}} + \frac{\rho_{green}}{\rho_{swir1} + \rho_{green}} \right]}{\frac{2\rho_{swir1}}{\rho_{swir1} + \rho_{nir}} + \left[\frac{\rho_{nir}}{\rho_{nir} + \rho_{red}} + \frac{\rho_{green}}{\rho_{swir1} + \rho_{green}} \right]} \quad (10)$$

where ρ_{blue} denotes the blue band, ρ_{green} denotes the green band, ρ_{red} denotes the red band, ρ_{nir} denotes the near-infrared band, and ρ_{swir1} denotes the short-infrared band 1.

- Heat

The LST can reflect the energy flow and material exchange in the soil–vegetation–atmosphere system. Therefore, the heat indicator is expressed using the LST. It can be retrieved using the atmospheric correction method.

The brightness of the thermal infrared radiation received by the satellite sensor is L_λ (Equation (11)):

$$L_\lambda = [\varepsilon \times B(LST) + (1 - \varepsilon)L_\downarrow] \times \tau + L_\uparrow \quad (11)$$

where ε denotes the land surface emissivity, which needs to be calculated using vegetation coverage; LST denotes the land surface temperature; $B(LST)$ denotes the black-body thermal radiation brightness; and L_\uparrow , L_\downarrow , τ denote the upward radiation, downward radiation and transmittance of the atmosphere in the thermal infrared band, which can be calculated using NASA atmospheric calculator to obtain the atmospheric profiles (<http://atmcorr.gsfc.nasa.gov/> (accessed on 28 August 2022)).

On this basis, the radiative brightness $B(LST)$ of a blackbody at temperature T in the thermal infrared band can be further obtained (Equation (12)). Then, the true LST can be obtained according to the inverse function of Planck’s formula (Equation (13)):

$$B(LST) = [L_{\lambda} - L_{\uparrow} - \tau(1 - \varepsilon)L_{\downarrow}] / (\tau \times \varepsilon) \tag{12}$$

$$LST = K_2 / \ln\left(\frac{K_1}{B(LST)} + 1\right) - 273 \tag{13}$$

For ETM+, $K_1 = 666.09 \text{ W}/(\text{m}^2 \cdot \mu\text{m} \cdot \text{sr})$, and $K_2 = 1282.71 \text{ K}$. For OLI Band 10, $K_1 = 774.89 \text{ W}/(\text{m}^2 \cdot \mu\text{m} \cdot \text{sr})$, and $K_2 = 1321.08 \text{ K}$.

2.3.3. Analysis of the Impact of LUCC on Ecological Quality

As a spatial statistical model, GeoDetector provides an approach to reveal the impact factors and drivers behind the spatial differentiation of geographic phenomena without making linear assumptions [47]. GeoDetector contains four modules: factor detection, ecological detection, interaction detection and risk detection. In this study, the factor detection module and the interaction detection module were coupled with the abundance index-based spatial heterogeneity quantification method to reveal the impacts and driving effects of LUCC on ecological quality.

- Factor Detection

The factor detection module mainly uses q -value (Equations (14)–(16)) to detect the extent to which the impact factor explains the spatial differentiation of geographical phenomena. The q ranges from $[0, 1]$, and the larger the q , the stronger the explanatory power of factor X for dependent variable Y and vice versa.

$$q = 1 - \frac{\sum_{h=1}^L N_h \sigma_h^2}{N \sigma^2} = 1 - \frac{SSW}{SST} \tag{14}$$

$$SSW = \sum_{h=1}^L N_h \sigma_h^2 \tag{15}$$

$$SST = N \sigma^2 \tag{16}$$

where $h = 1, \dots, L$ is the stratification of dependent variable Y or factor X ; N_h and N denote the number of cells in the stratification h and the whole region, respectively; σ_h^2 and σ^2 denote the variance of variables in the stratification h and the whole region, respectively; and SSW and SST denote the sum of variance within stratifications and the total variance of the whole region, respectively.

- Interaction Detection

The interaction detection module is designed to identify interactions between different factors X , i.e., to assess whether two factors acting in synergy increase or decrease the explanatory power on the dependent variable Y or whether the effects of these factors on the dependent variable Y are independent of each other. The interaction types are shown in Table 2.

Table 2. Interaction detection types.

Interaction Relations	Interaction Types
$q(X_1 \cap X_2) < \text{Min}(q(X_1), q(X_2))$	Nonlinear weaken
$\text{Min}(q(X_1), q(X_2)) < q(X_1 \cap X_2) < \text{Max}(q(X_1), q(X_2))$	Univariable weaken
$q(X_1 \cap X_2) > \text{Max}(q(X_1), q(X_2))$	Bivariable enhanced
$q(X_1 \cap X_2) = q(X_1) + q(X_2)$	Independent
$q(X_1 \cap X_2) > q(X_1) + q(X_2)$	Nonlinear enhanced

- Impact Factors and Discretization Method

In this study, six LULC types, FL, WL, GL, WB, UL and BA, were taken as the impact factors X and RSEI as the dependent variable Y to detect the controlling effects of the spatial distribution of different LULCs on the spatial pattern of ecological quality in Jinan City. In addition, the mutual transfer among the six LULCs were taken as the impact factors X , and the changes in RSEI were taken as the dependent variable Y to reveal the driving effects of the spatial distribution of LUCC on the changes in ecological quality.

To achieve the above objectives, we need to decompose the mixed LULCs or LUCCs into single types. However, the decomposed results only have spatial distribution and not spatial heterogeneity. Therefore, here, we proposed a type decomposition and spatial heterogeneity quantification method based on the abundance index. First, the study area was divided into grids using a spatial up-scaling approach. Then, the abundance of the factors X was numerically quantified by counting the area of LULCs or LUCCs within each grid. In addition, a typological preprocessing of the abundance calculation results was implemented as the impact factors input into GeoDetector were required to be typological quantities. Here, the natural breaks method was used to reclassify the factor quantification results into five levels to generate the hierarchy or classification. To eliminate the spatial scale differences between the impact factors X and the variables Y , we completed the spatial up-scaling using the same grid for the mean statistics of the variables Y . In this way, we established the spatial pairwise correspondence between the factors and the variables using the grid as the unit of analysis. Finally, they were input into GeoDetector for analysis. The whole process is shown in Figure 2.

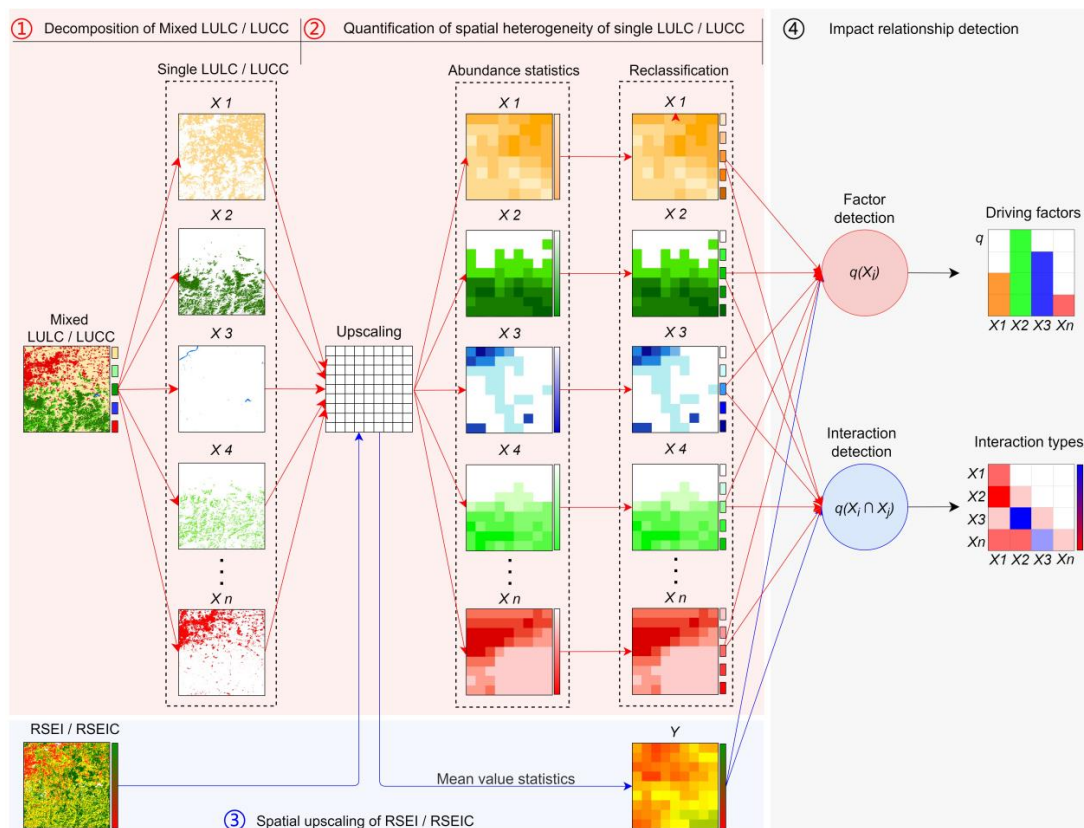


Figure 2. Discretization process of the factors. LULC/LUCC are land use/land cover or land use/land cover change. X_1, X_2, \dots, X_n denote impact factors, which are single types decomposed from the mixed LULC/ LUCC and are ultimately typological quantities. RSEI/RSEIC denote variables Y , which are ecological quality or changes in ecological quality and are numerical quantities.

3. Results

3.1. Spatio–Temporal Changes of LULC in Jinan City

The classification results (Figure 3) showed that the spatial pattern of LULCs in Jinan is very distinct. The northern and eastern parts of the Yellow River are relatively flat and mainly dominated by FL. In the southern parts of the Yellow River, the main LULCs are BA, WL and GL. The constraining effects of the Yellow River and topography on the spatial pattern of LULCs were significant. The structure of LULC in Jinan City has not changed significantly in the past 20 years, in general, and is still dominated by FL and BA with a proportion of over 70%, whereas the proportion of WL, GL, WB and other types with significant ecological regulations was relatively low. However, the area of each LULC in Jinan City has changed dramatically in the past 20 years. Of which, the areas of FL and GL showed an obvious decreasing trend, whereas the areas of BA and WB showed a clearly increasing trend. The area of WL decreased first and then increased, whereas the area of UL showed the opposite, and both showed fluctuating changes.

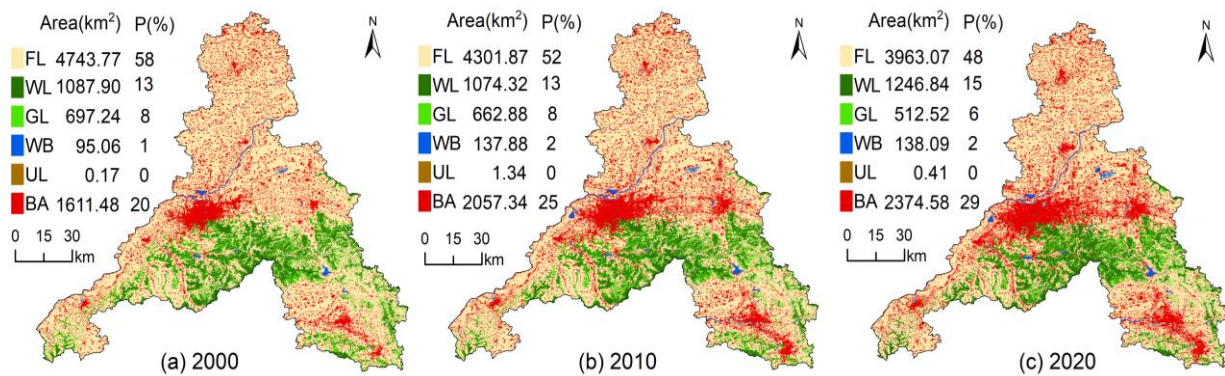


Figure 3. Classification results of land use/land cover in Jinan City: (a) is the land use/land cover structure and spatial distribution in 2000; (b) is the land use/land cover structure and spatial distribution in 2010; and (c) is the land use/land cover structure and spatial distribution in 2020.

In addition, the LULC in Jinan underwent very complex and uneven transfers in the structural and spatial distribution in the last 20 years (Figures 4 and 5). Therein, urban expansion occupied a large amount of FL, WL, GL and WB, resulting in a 47% increment in the area of BA. The urban expansion was accompanied by the reclamation of WL, GL and WB, and this occurred mainly in the southern mountainous areas where a large amount of WL, GL and WB transferred to FL. However, after the introduction of the ecological protection policy of “grain for green” in 2003, a lot of FL in the southern mountainous areas transferred to WL and GL. In particular, the total area of WL has increased by 225.598 km² in the last decade, of which 51% was contributed by the transfer of FL. Overall, urban expansion intensified the transfer of surrounding FL to BA. The implementation of farmland reclamation and ecological protection policies prompted WL, GL, WB and UL to exhibit a high degree of dynamics.

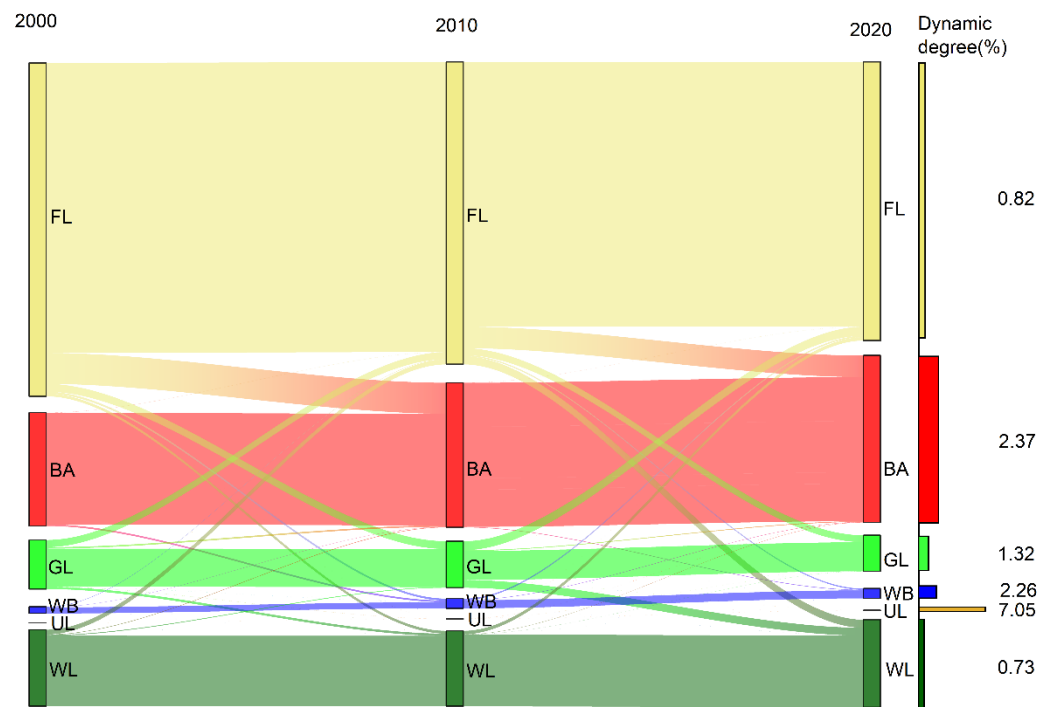


Figure 4. Transfer flow and dynamic degree of land use/land cover in Jinan. Yellow denotes farmland, red denotes built-up areas, light green denotes grassland, blue denotes water body, brown denotes unutilized land, and dark green denotes woodland.

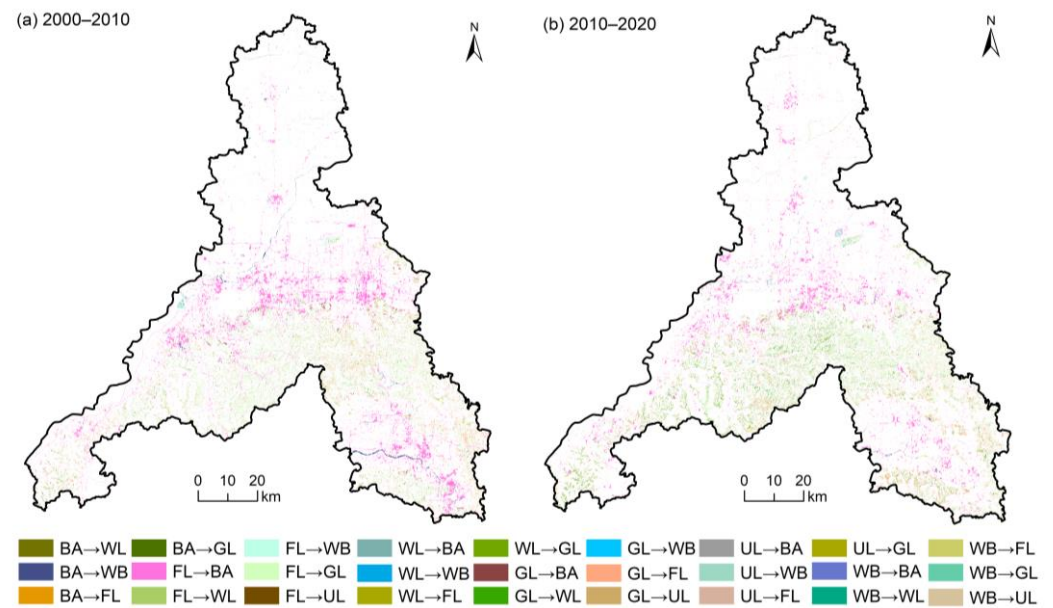


Figure 5. Spatial distribution of land use/land cover transfers in Jinan from 2000 to 2020: (a) shows the transfer results in the first decade; (b) shows the transfer results in the second decade.

3.2. Response of Ecological Quality to LUCC in Jinan City

The PCA results (Tables 3–5) show that the contribution rate of the first principal component is 82.10% in 2000, 83.44% in 2010 and 80.17% in 2020, which contains the information of the most indicators and is effectively representative of the regional ecological quality status. The calculation results of the first principal component for the three periods were normalized to obtain the spatial distribution of RSEI in Jinan. Then, in order to facilitate the analysis and evaluation, the RSEI was further divided into five levels: poor (0–0.2), fair (0.2–0.4), moderate (0.4–0.6), good (0.6–0.8) and excellent (0.8–1).

Table 3. Principal component analysis results of remote sensing ecological index in 2000.

	PC1	PC2	PC3	PC4
NDVI	0.751	−0.189	0.360	0.520
WET	0.363	0.323	−0.854	0.184
NDBSI	−0.548	0.058	−0.032	0.834
LST	−0.061	−0.925	−0.374	0.011
Eigenvalue	0.259	0.029	0.026	0.002
Contribution rate (%)	82.10	9.20	8.10	0.60
Cumulative contribution rate (%)	82.10	91.30	99.40	100

Table 4. Principal component analysis results of remote sensing ecological index in 2010.

	PC1	PC2	PC3	PC4
NDVI	0.699	0.169	−0.437	−0.539
WET	0.008	−0.148	−0.785	0.601
NDBSI	−0.713	0.212	−0.435	−0.507
LST	−0.035	−0.951	−0.052	−0.303
Eigenvalue	0.267	0.041	0.009	0.002
Contribution rate (%)	83.44	12.87	2.93	0.76
Cumulative contribution rate (%)	83.44	96.31	99.24	100

Table 5. Principal component analysis results of remote sensing ecological index in 2020.

	PC1	PC2	PC3	PC4
NDVI	0.757	−0.181	0.338	0.529
WET	0.304	0.918	−0.250	0.039
NDBSI	−0.555	0.307	0.539	0.555
LST	−0.163	−0.172	−0.730	0.641
Eigenvalue	0.249	0.048	0.011	0.003
Contribution rate (%)	80.17	15.56	3.24	1.04
Cumulative contribution rate (%)	80.17	95.72	98.96	100

The results of the RSEI calculation in Jinan (Figure 6) show that the overall ecological quality of Jinan City shows a decreasing trend from 2000 to 2020. Of which, the area with excellent and good ecological quality declined sharply, reaching 25.4 and 23.7%, respectively. The area with moderate ecological quality remained relatively stable, and the area with fair ecological quality increased by 26.7%, whereas the area of poor ecological quality in 2020 is 2.4 times of that in 2000. From the spatial distribution of RSEI in each year (Figure 6a–c), it can be seen that the better ecological quality of Jinan is mainly distributed in the southern mountainous area and the northern plain area, whereas the ecological quality located in the central urban area and the town centers of counties and districts is poor. The overall ecological quality in the central urban area of Jinan was increasingly degraded and developed in an east–west strip, but the overall ecological quality in the southern mountainous area was improved.

The spatial distribution of ecological quality in Jinan, which underwent obvious relative changes between the two decades, is shown in Figure 7. The areas where ecological quality declined from 2000 to 2010 were distributed throughout Jinan. Of these areas, the degradation of ecological quality was particularly serious in the central part of Shanghe County, whereas the ecological quality improved in the northern part of Shanghe County and the eastern part of Laiwu District. From 2010 to 2020, the spatial differentiation of the ecological quality change pattern in Jinan City was more obvious. The ecological quality in the northern, southwestern and southeastern parts of Jinan was more severely degraded, whereas the ecological quality in the northern part of the Yellow River, the contiguous areas along the Yellow River and the southern mountainous areas were all improved. Collectively, there was a strong spatial inconsistency between the changes in ecological quality in the first and second decades of Jinan City. In addition, the statistical results (Figure 7) show that the area of both improved and degraded ecological quality in Jinan City was increased, and the trend of polarization intensified significantly.

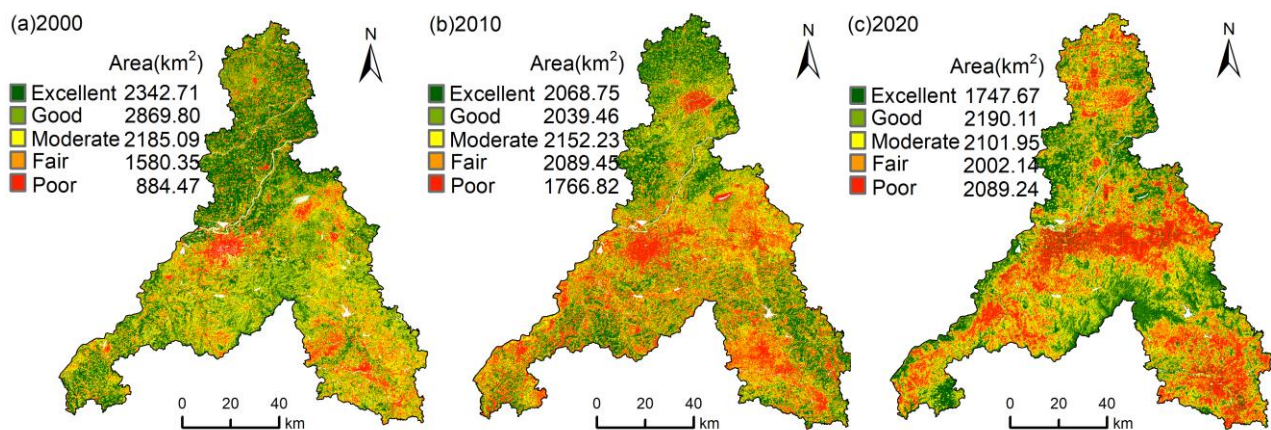


Figure 6. Spatial distribution of ecological quality in Jinan from 2000 to 2020: (a) is the structure and spatial distribution of ecological quality in 2000; (b) is the structure and spatial distribution of ecological quality in 2010; and (c) is the structure and spatial distribution of ecological quality in 2020.

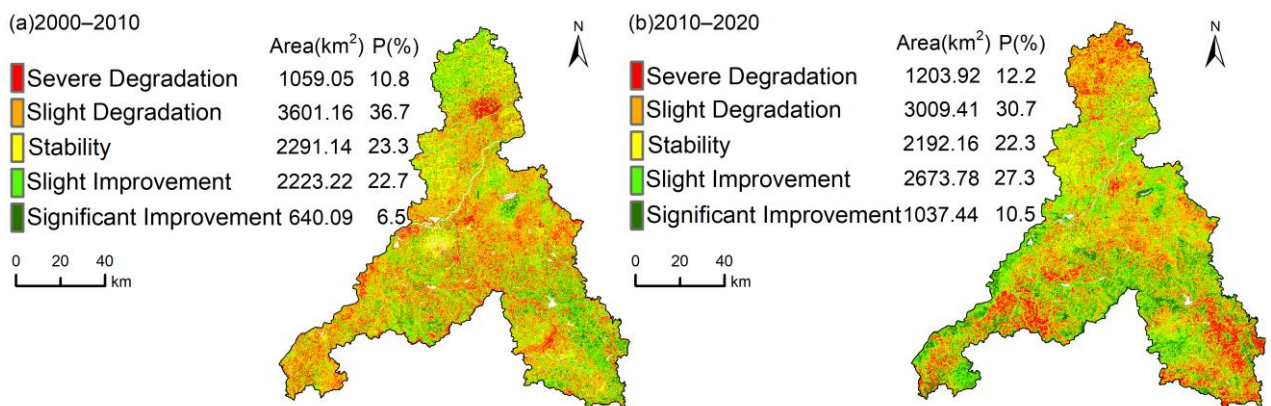


Figure 7. Spatial distribution of ecological quality changes in Jinan from 2000 to 2020: (a) shows the ecological quality changes in the first decade; (b) shows the ecological quality changes in the second decade.

3.3. Control Effects of LULC on the Spatial Pattern of Ecological Quality in Jinan City

The scale effects generated by the spatial upscaling method need to be considered in the factor discretization process to seek the optimal analysis scale. Therefore, we conducted experiments on the scale effects between 0.5 and 8 km using the factor detection module of GeoDetector at 0.5 km intervals. The experimental results (Figure 8) show that the q -values of the impact factors began to level off after 2 km and tended to fluctuate again after 4.5 km, indicating the lack of adaptability of the scales outside [2–4.5] km. The results of significance tests (p -values) within [2–4.5] km showed that the q -values of the two main LULCs, FL and WL, were not significant after the scale of 3 km, and the q -values of each factor reached the maximum at 3 km. Therefore, 3 km was adopted as the optimal analysis scale in this study. Then, we performed factor and interaction detection of the ecological quality spatial patterns after discretizing the RSEI and LULCs for 2000–2020 at the optimal scale.

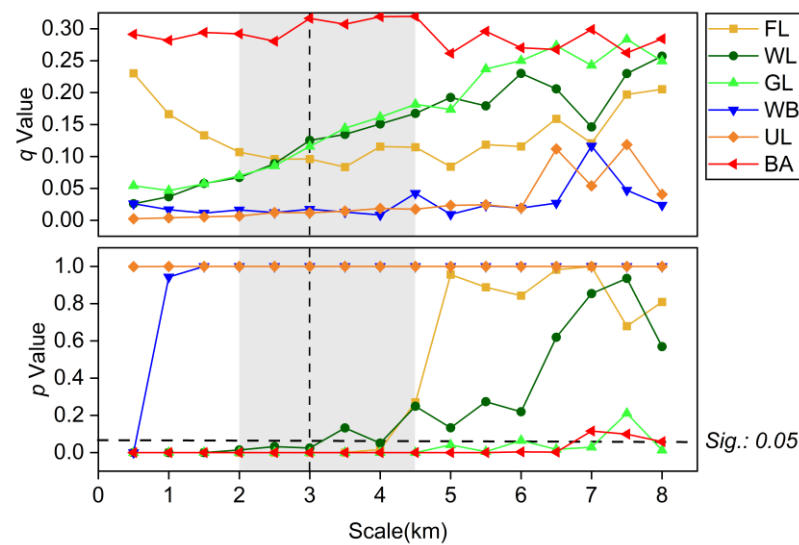


Figure 8. Scale effects of land use/land cover impact on ecological quality. $p < 0.05$ indicates a significant detection result.

The results of the factor detection (Figure 9) show that the explanatory power of the LULC distribution on the spatial pattern of ecological quality was slightly different in the three years. In a comprehensive comparison, the order of the controlling effect of LULC distribution on the spatial pattern of ecological quality in Jinan was $BA > WL > GL > FL > WB > UL$. Of which, the area of BA occupied a considerable proportion and was the main factor controlling the spatial pattern of ecological quality in Jinan. WL and GL have important ecological service functions and were key factors in maintaining the ecological quality of Jinan City. Although the anthropogenic intervention of FL was more intense, crops have dense growth spacing and abundant biomass, which were also important factors to maintain the ecological quality of Jinan City. In comparison, the area of WB and UL were relatively small and had weaker impacts on the overall spatial pattern of ecological quality in Jinan, but they were still factors that cannot be ignored in influencing regional ecological quality. From the perspective of temporal development, the q -values of most of the impact factors showed fluctuating change characteristics. However, the overall trend showed that the controlling effects of BA and FL on the spatial pattern of ecological quality tended to decrease over the last 20 years, whereas the influences of WL, GL, WB and UL tended to increase.

The interaction detection results (Figure 10) show that most of the interactions among LULCs in the three years were nonlinearly enhanced, and a few were bivariable-enhanced, with no independent and weakened relationships. This indicates that the interactions among the LULCs all have enhanced effects on the spatial pattern of ecological quality in Jinan, and all of them are greater than the influence of each single LULC. Overall, $BA \cap WL$ had the strongest explanatory power for the spatial pattern of ecological quality in Jinan, whereas $BA \cap GL$ and $BA \cap FL$ hold the second and third positions, respectively. Next, $FL \cap GL$ and $FL \cap WL$ also had strong explanatory power, taking up the fourth and fifth positions, respectively. The top five interaction types of explanatory power in the past 20 years also showed fluctuating change characteristics, but the overall trend was decreasing. In particular, the influence of the interaction between BA and other types on the spatial pattern of ecological quality declined significantly. In contrast, the influences of interactions among WL, GL, WB and UL on the spatial patterns of ecological quality increased significantly.

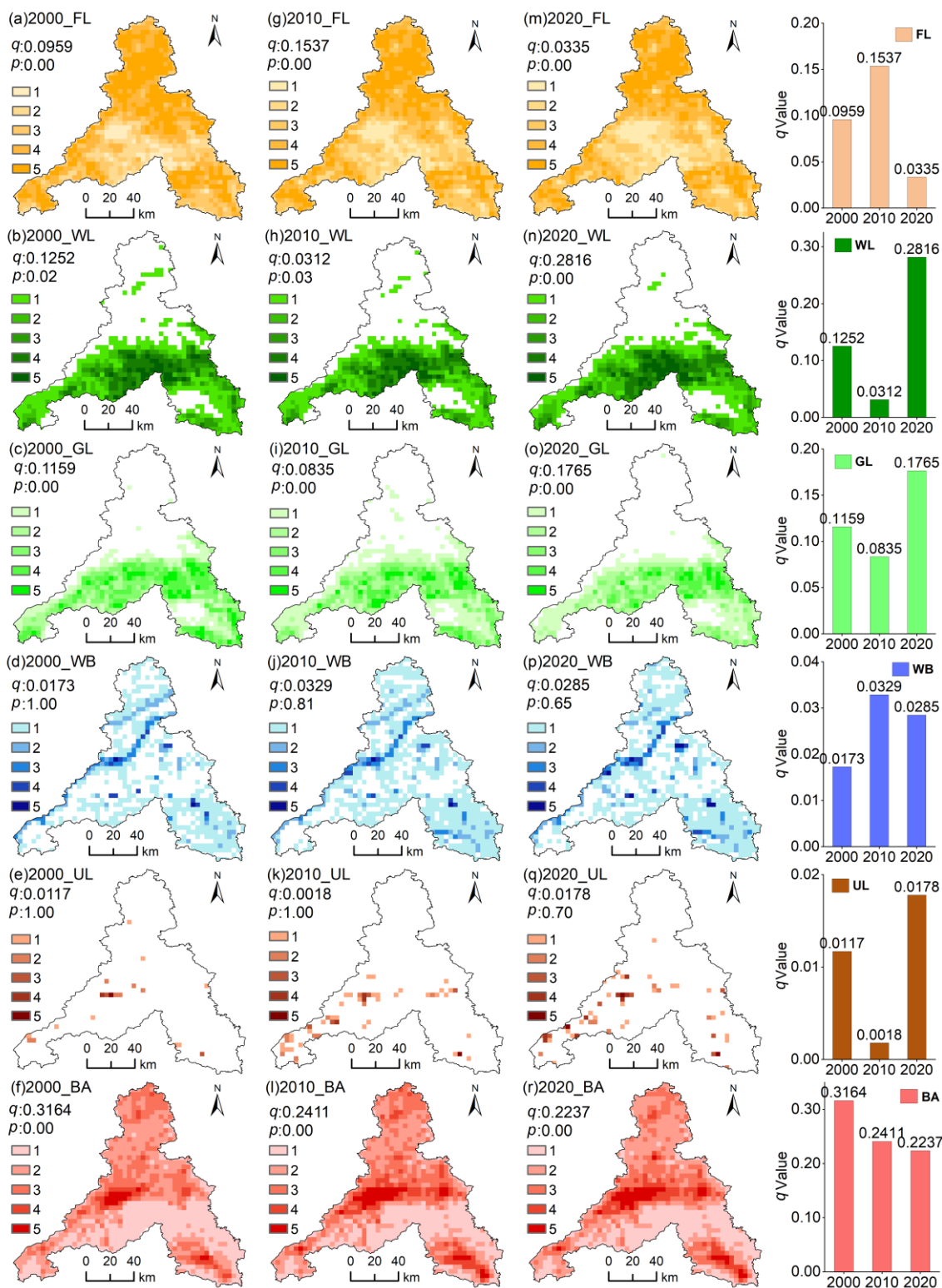


Figure 9. Spatial distribution of impact factors and factor detection results: (a–f) are the spatial distribution of impact factors and factor detection results in 2000; (g–l) are the spatial distribution of impact factors and factor detection results in 2010; (m–r) are the spatial distribution of impact factors and factor detection results in 2020. The rightmost column displays the variation in q -value of each impact factor with years.

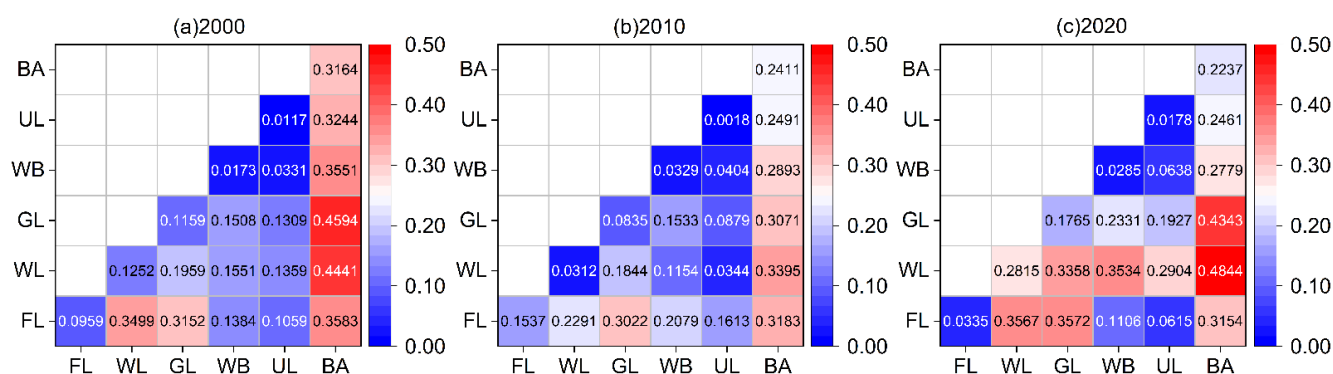


Figure 10. Interaction detection results of factors affecting the spatial pattern of ecological quality: (a) is the interaction detection result in 2000; (b) is the interaction detection result in 2010; and (c) is the interaction detection result in 2020. The redder color in the figure indicates the stronger interaction between the two impact factors and vice versa.

3.4. Driving Effects of LUCC on Ecological Quality Changes in Jinan City

To further reveal the driving effects of LUCC on ecological quality changes in Jinan, we discretized LUCC and RSEI changes from 2000 to 2010 and 2010 to 2020, respectively, based on an optimal analysis scale and conducted factor and interaction detection of this change process again using GeoDetector.

The factor detection results are shown in Figures 11 and 12. From 2000 to 2010, the order of factors that significantly drive ecological quality changes in Jinan was $GL \rightarrow FL > FL \rightarrow BA > GL \rightarrow WL > FL \rightarrow GL > BA \rightarrow WB$. From 2010 to 2020, the order was $WL \rightarrow FL > GL \rightarrow WL > FL \rightarrow GL > FL \rightarrow GL > FL \rightarrow WL > WL \rightarrow BA$. However, we also found that the driving effects of individual LUCCs on the ecological quality changes were all weak.

Subsequently, we selected the factors with positive and negative impacts on the ecological quality changes separately for interaction detection. The results (Figure 13) show that the interactions of all factors on the ecological quality changes were enhanced, and the coupling of multiple LUCCs had strong driving effects on the ecological quality changes. This indicates that the ecological quality changes in Jinan were the result of the co-action of multiple LUCCs.

Therein, the interactions between $GL \rightarrow WL$, $FL \rightarrow GL$, $FL \rightarrow WL$ and $BA \rightarrow WB$ all had stronger explanatory power for the improvement of ecological quality in the first decade (Figure 13a). This indicates that the transfer of GL and FL to WL, the transfer of FL to GL and the area increase in WB in some regions during the first decade enhanced the greenness and wetness, which have collectively contributed to the development of a better ecological quality. In addition, $FL \rightarrow BA \cap GL \rightarrow FL$ had the strongest explanatory power for the ecological quality degradation during this period (Figure 13b). This suggests that the occupation of large amounts of FL by urban expansion and the reclamation of large amounts of GL into FL raised the regional heat and dryness, which exacerbated the degradation of ecological quality during this period.

In comparison, $GL \rightarrow WL \cap FL \rightarrow WL$ had the strongest explanatory power for the ecological quality improvement in the second decade (Figure 13c). This indicates that the transfer of GL and FL to WL was still the main driver of ecological quality improvement in this period. The interaction between the two greatly enhanced regional greenness and contributed to the improvement of ecological quality. In addition, $WL \rightarrow FL \cap WL \rightarrow BA$ had the strongest explanatory power for ecological quality degradation in the second decade (Figure 13d), and the transfer of WL to FL and BA reduced regional greenness and enhanced regional dryness and heat, which cooperatively exacerbated ecological quality degradation.

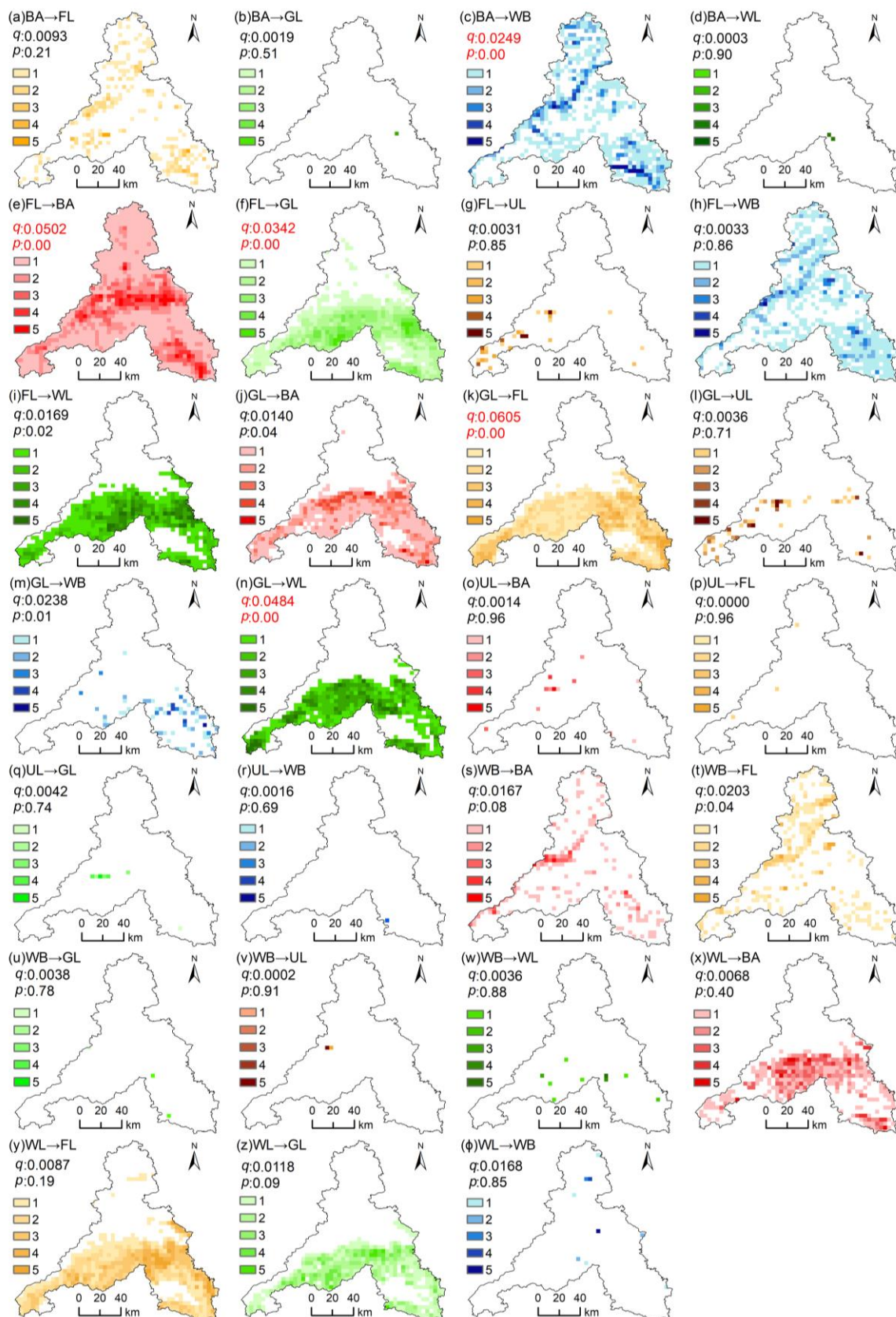


Figure 11. Factor detection results of ecological quality changes from 2000 to 2010: (a–φ) show the spatial distribution of land use/land cover transfers from 2000 to 2010, respectively. The q and p values in each figure indicate the explanatory power and significance of that spatial distribution on ecological quality changes.

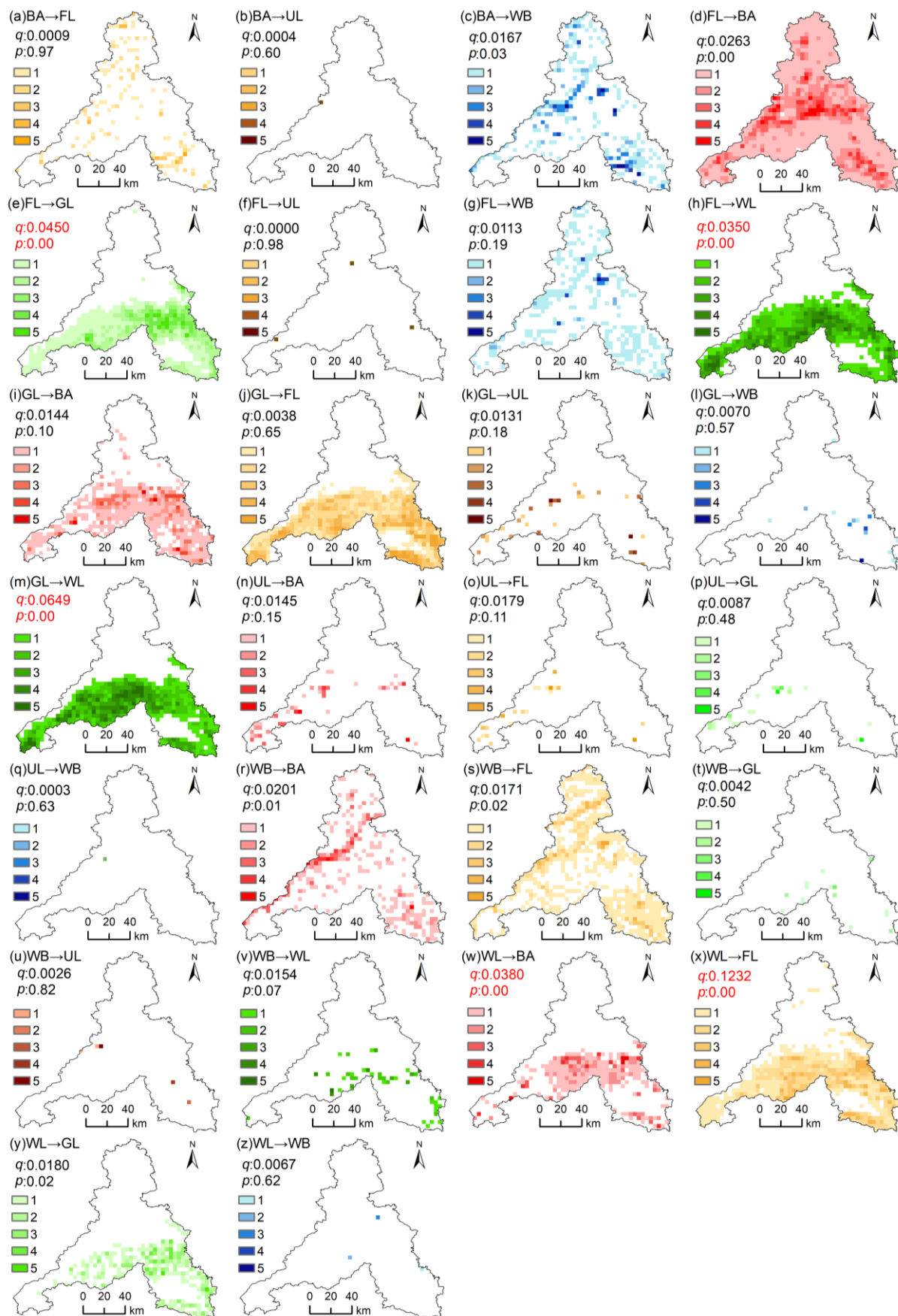


Figure 12. Factor detection results of ecological quality changes from 2010 to 2020: (a–z) show the spatial distribution of land use/land cover transfers from 2010 to 2020, respectively. The q and p values in each figure indicate the explanatory power and significance of that spatial distribution on ecological quality changes.

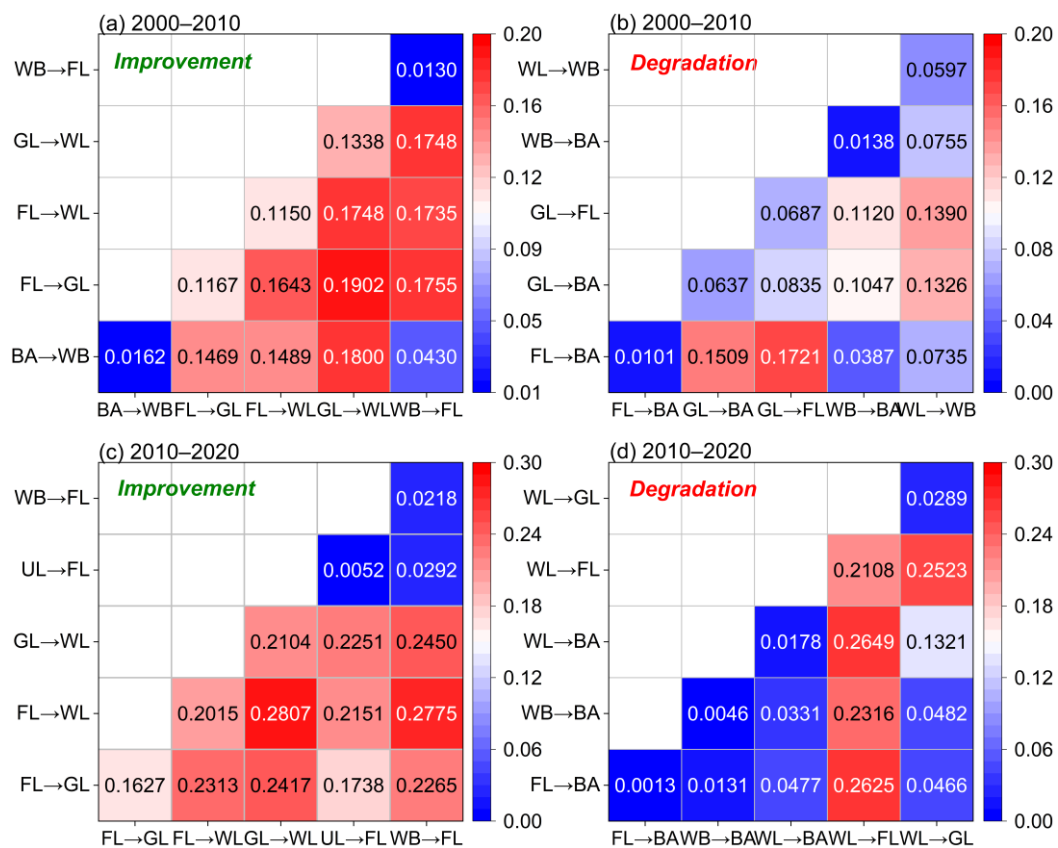


Figure 13. Interaction detection results of drivers of ecological quality changes from 2000 to 2020: (a,b) are the interaction detection results of drivers of ecological quality improvement and degradation from 2000 to 2010, respectively; (c,d) are the interaction detection results of drivers of ecological quality improvement and degradation from 2010 to 2020, respectively. The redder color indicates the stronger interaction between the two factors, and the bluer color indicates the weaker interaction between the two factors.

4. Discussion

4.1. Coupled Impact of Land Requirements and Policies on LULC and Ecological Quality Changes at Different Stages of Urbanization

The spatial distribution of LULC in Jinan had a distinct pattern and was dominated by FL and BA, whereas LULCs with important ecological service functions, such as WL, GL and WB, accounted for a relatively low proportion (Figure 3). The structure of LULCs in Jinan did not greatly changed during the development process in the past 20 years, but more complex transfers occurred among LULCs (Figures 4 and 5). This is mainly influenced by the land requirements and policies at different stages of development in Jinan. In the first decade, Jinan City was in a period of rapid urbanization. Urban construction required a large amount of land supply in the surrounding areas, and, therefore, inevitably occupied a large amount of FL [48]. At the same time, in order to maintain the FL area, the “Requisition-Compensation Balance” [49,50] was maintained mainly by means of suburban land reclamation, such as “reclaiming land from lakes”, “reclaiming land from riverbeds” and “deforestation for farmland”. Although this “Requisition-Compensation Balance” policy of FL is significant for maintaining food security, it also makes the new FL subject to natural disasters and ecological risks such as soil erosion and flooding [50,51]. In the second decade, the growth rate of Jinan’s urban expansion had slowed down, but it also still occupied a considerable area of the surrounding FL. As a result, there was still a large amount of WL, GL and WB transferred to FL to maintain its scale. In addition, as the ecological protection and restoration projects were in the upper and middle Yellow River basin [52–54], the ecological protection policy of “Grain for Green”, implemented by

Jinan City, allowed a large amount of FL transferred to GL and WL in the past 20 years. This policy has made an important contribution to the improvement of vegetation cover, ecosystem function and biodiversity conservation in Jinan and the whole downstream of the YRB.

With the changes in LULC in Jinan, the overall ecological quality showed a decreasing trend in the past 20 years, and the area of poor ecological quality increased about 1.4 times. Moreover, the spatial pattern of ecological quality in Jinan experienced a change from fragmented heterogeneity to zonal heterogeneity. In particular, the spatial agglomeration effect of ecological quality degradation in the central urban area of Jinan got more and more serious and gradually showed an obvious east–west belt-shaped distribution (Figure 6). On the one hand, this is because a large number of impervious surfaces were built during the rapid urbanization [24,41], leading to the deterioration of ecological quality in the central urban area. On the other hand, Jinan City is restricted by the “Ecological Protection Red Line” of the Yellow River and the southern mountainous area during the urbanization process and has implemented the urban spatial development strategy of “Expanding Eastward and Advancing Westward”. Although, Ren et al. [17] argued that Jinan City has a high coupling degree from the perspective of urbanization and eco-efficiency and is basically sustainable, the spatial agglomeration effect of ecological quality degradation will diminish the ecological service capacity of existing habitats and also increases the resistance to ecological processes such as species migration. Therefore, while leading the economic development of the lower reaches of the YRB, Jinan City also suffers from declining ecological service capacity and blocked ecological process cycles and still faces greater challenges in achieving SDG 11 and SDG 15, the sustainable development goals advocated by the United Nations.

Compared with the spatial pattern of ecological quality, there was no obvious regularity in the spatial distribution of ecological quality improvement and degradation in Jinan. However, it showed significant spatial inconsistency between the first and the second decade, and the trend of polarization in the ecological quality in the second decade strengthened obviously (Figure 7). Although, the response of ecological quality to LUCC was more complex in both periods, there were obvious differences in the driving factors involved behind it. In the first decade, the policy of “Grain for Green” was the main factor for the ecological quality improvement in Jinan, whereas the occupation of FL by urban expansion and the reclamation of GL were the main drivers of ecological quality degradation (Figures 11 and 13). In the second decade, the policy of “Grain for Green” was still the main factor for the ecological quality improvement, but the urban expansion and the transfer of WL to FL became the major drivers of ecological quality degradation (Figures 12 and 13). This is mainly due to the fact that the FL maintenance policy of “Requisition–Compensation Balance” in the process of urban expansion has faced many challenges in its actual implementation [48,49]. To guard the red line of FL protection, Jinan City implemented the policy of “Returning Forest to Farming”, which resulted in the transfer of a large amount of WL to high-quality FL. This is different from what has been advocated in the existing study about adhering to the conservation red line of WL to maintain its ecological service function and avoid WL reclamation [17]. Accordingly, the policy shift from the synergy of “ecological conservation and farmland maintenance” to the synergy of “ecological conservation and farmland protection” during urbanization has resulted in different ecological quality response characteristics in Jinan over the two decades.

4.2. Proposals for Urban Land Development and Ecological Protection

It is foreseeable that the area of land available for afforestation and ecological restoration will become more and more limited in the future. Therefore, the Jinan government should seek a balance between urbanization and ecological protection by means of high-quality land development and spatial layout optimization. For one thing, it is suggested that Jinan City should strengthen the efficient and intensive utilization of land, strictly control the expansion of production land and living land and improve the quality of devel-

opment. This will reduce the occupation of FL, WL, GL and WB through the expansion of BA, thus contributing to slowing down the further expansion of the spatial agglomeration effect of ecological quality degradation. In addition, it is suggested that Jinan City adopts the strategy of urban–rural gradient spatial zoning to strengthen the protection, restoration and planning of blue–green ecological spaces, integrate the protection of WL, GL and WB with urban construction and optimize the layout of urban ecological spaces. Firstly, the exposure and ecological quality of existing blue and green spaces in urban areas to citizens should be improved, which will help to reduce the urban heat island effect and improve the equity of urban habitat quality [55,56]. Secondly, the construction of ecological infrastructure in urban–rural combination areas should be promoted, which will help to reduce the ecological resistance of urban space [57] and promote the cyclic exchange of ecological processes in urban–rural gradients [58,59]. Then, the restoration and planning of suburban ecological reserves should be strengthened, which will clarify the spatial boundaries for future urban development and maintain the spatial structure of overall ecological quality.

4.3. Limitations and Prospects

LULC is the direct factor that affects ecological quality. The physical properties of different LULCs determine that their changes will alter the ecological covariates such as greenness, wetness, dryness, and heat, which are directly related to human perceptions. Therefore, this study focused on the LUCC and its ecological quality response relationships during the urbanization of Jinan City and revealed the driving mechanisms of LUCC on ecological quality changes arising from land requirement changes and policy impacts in different periods. This will provide references for urban development quality assessment studies in the lower YRB, land and ecological conservation policy studies and the achievement of the United Nations Sustainable Development Goals (SDG 11 and SDG 15). However, this study only explored the relationship of ecological quality in response to the mutual transfer between the six LULCs, which may ignore the impact of changes in other, more refined LULCs on ecological quality. For example, the southern region of Shanghe County was always FL and did not transfer to BA, but a significant portion of the area underwent severe ecological quality degradation (Figure 5). This is mainly because this region is a special agricultural planting area in Shanghe County, with garlic mainly grown on a large scale, and the size of the planting area expanded rapidly to 133 km² after 2006. In this region, garlic is harvested in May–June and sown in September–October. This results in low surface vegetation cover in this region during the study period, and the final inversion of RSEI is low due to the plastic mulch planting technique used, which reduces surface wetness and increases surface temperature. Therefore, in future studies, we will include more refined LULC or region-specific factors in the exploration of driving mechanisms.

In fact, LUCC will also change landscape patterns [60,61]. At a regional or mesoscopic scale, changes in patch structure, shape, size and type will alter the antagonistic and synergistic effects of different ecological covariates, which will indirectly affect the overall ecological quality. For instance, the expansion of the central urban area of Jinan has caused the structural simplification and spatial homogenization of regional patches to become increasingly serious, which, in turn, triggers the spatial clustering effect of ecological quality degradation (Figure 6). This has been confirmed in some of our research results. Likewise, the fragmentation and heterogeneity of landscapes with important ecological services can have important implications for changes in ecological quality. In this study, we only partially analyzed and explored this aspect from a qualitative perspective. Therefore, our next task will be to continue to study in-depth the influence mechanism and threshold effect of urban landscape pattern changes on ecological quality changes in order to provide a more comprehensive reference for decision-making on high-quality development and ecological conservation in the YRB.

5. Conclusions

Land use/land cover change is the most critical factor affecting ecological quality in the urbanization process. Exploring its impact mechanism will be beneficial to the rational formulation of urban development and ecological protection policies and strategies. In this study, Jinan, a megacity, was selected as a typical region to explore the land use/land cover change and its ecological impacts on cities in the lower Yellow River basin. The change in the ecological quality in Jinan City was retrieved using the remote sensing ecological index based on Landsat images in 2000, 2010 and 2020. Then, the mixed-type decomposition and spatial heterogeneity quantification of land use/land cover change were addressed using the abundance index. On this basis, the impact mechanism of land use/land cover change on ecological quality in the past 20 years was revealed using GeoDetector. The results show that: The spatial pattern of ecological quality was mainly controlled by built-up areas and farmland. Changes in land requirements and policies during the last 20 years of urbanization led to very complex transfers between land use/land cover types, which, in turn, led to very different spatio-temporal response characteristics of ecological quality. In particular, urban expansion and farmland protection prompted the transfer of farmland and woodland to built-up areas and the transfer of grassland and woodland to farmland as the main factors that exacerbated the degradation of regional ecological quality. Meanwhile, the introduction of ecological protection policies prompted the transfer of farmland to woodland and grassland as the main reason for promoting the improvement of regional ecological quality. Although, ecological protection policies were implemented, in parallel with urban expansion, during the urbanization process, the uneven structure and spatial distribution of land use/land cover changes led to a decreasing trend in overall ecological quality and an increasingly serious spatial agglomeration effect. Therefore, it is suggested to achieve the balance between urbanization and ecological conservation by coupling and synergizing high-quality land development and spatial layout optimization. In future research work, we will focus on the impact of landscape pattern changes on ecological quality, with a view to providing a more comprehensive scientific reference for the ecological conservation and high-quality, sustainable development of cities in the Yellow River basin.

Author Contributions: Conceptualization, G.Y. and Q.W.; methodology, T.L. (Tongwen Liu); software, T.L. (Tao Li); validation, X.L., Y.F. and G.S.; formal analysis, G.Y. and Q.W.; investigation, X.L. and Y.F.; resources, X.L., Y.F. and G.S.; data curation, X.L., Y.F. and G.S.; writing—original draft preparation, G.Y. and Q.W.; writing—review and editing, T.L. (Tongwen Liu) and Q.W.; visualization, T.L. (Tao Li); supervision, T.L. (Tao Li); project administration, G.Y., T.L. (Tongwen Liu) and Q.W.; funding acquisition, G.Y., T.L. (Tongwen Liu) and Q.W. All authors have read and agreed to the published version of the manuscript.

Funding: This research was funded by “Ph.D. Programs Foundation of Shandong Jianzhu University, grant number XNBS1984” and “Science and Technology Innovation Project of Shandong Provincial Bureau of Geology and Mineral Resources, grant number KY201954”.

Data Availability Statement: Not applicable.

Acknowledgments: The authors are grateful to the USGS for providing the Landsat images, to the Geological and Mineral Exploration Information System of Shandong Province for providing the field survey data and interpreted sample data, and to the State Key Laboratory of Resources and Environmental Information System (SKLREIS), Institute of Geographic Sciences and Natural Resources Research, Chinese Academy of Sciences (IGSNRR, CAS) for providing the software technical support.

Conflicts of Interest: The authors declare no conflict of interest.

References

1. Feng, S.; Fan, F. Developing an Enhanced Ecological Evaluation Index (EEEI) Based on Remotely Sensed Data and Assessing Spatiotemporal Ecological Quality in Guangdong–Hong Kong–Macau Greater Bay Area, China. *Remote Sens.* **2022**, *14*, 2852. [[CrossRef](#)]
2. Airiken, M.; Zhang, F.; Chan, N.W.; Kung, H.-T. Assessment of spatial and temporal ecological environment quality under land use change of urban agglomeration in the North Slope of Tianshan, China. *Environ. Sci. Pollut. Res. Int.* **2022**, *29*, 12282–12299. [[CrossRef](#)] [[PubMed](#)]
3. Zhou, J.; Liu, W. Monitoring and Evaluation of Eco-Environment Quality Based on Remote Sensing-Based Ecological Index (RSEI) in Taihu Lake Basin, China. *Sustainability* **2022**, *14*, 5642. [[CrossRef](#)]
4. Zhang, T.; Yang, R.; Yang, Y.; Li, L.; Chen, L. Assessing the Urban Eco-Environmental Quality by the Remote-Sensing Ecological Index: Application to Tianjin, North China. *Isprs Int. Geo-Inf.* **2021**, *10*, 475. [[CrossRef](#)]
5. Xu, H.; Ding, F.; Wen, X. Urban Expansion and Heat Island Dynamics in the Quanzhou Region, China. *IEEE J. Sel. Top. Appl. Earth Observ. Remote Sens.* **2009**, *2*, 74–79. [[CrossRef](#)]
6. Zhang, S.; Yang, P.; Xia, J.; Qi, K.; Wang, W.; Cai, W.; Chen, N. Research and Analysis of Ecological Environment Quality in the Middle Reaches of the Yangtze River Basin between 2000 and 2019. *Remote Sens.* **2021**, *13*, 4475. [[CrossRef](#)]
7. Mustafa, A.; Szydlowski, M. The Impact of Spatiotemporal Changes in Land Development (1984–2019) on the Increase in the Runoff Coefficient in Erbil, Kurdistan Region of Iraq. *Remote Sens.* **2020**, *12*, 1302. [[CrossRef](#)]
8. An, M.; Xie, P.; He, W.; Wang, B.; Huang, J.; Khanal, R. Spatiotemporal change of ecologic environment quality and human interaction factors in three gorges ecologic economic corridor, based on RSEI. *Ecol. Indic.* **2022**, *141*, 109090. [[CrossRef](#)]
9. Xu, F.; Li, H.; Li, Y. Ecological environment quality evaluation and evolution analysis of a rare earth mining area under different disturbance conditions. *Environ. Geochem. Health* **2021**, *43*, 2243–2256. [[CrossRef](#)]
10. Lai, S.; Eladawy, A.; Sha, J.; Li, X.; Wang, J.; Kurbanov, E.; Lin, Q. Towards an integrated systematic approach for ecological maintenance: Case studies from China and Russia. *Ecol. Indic.* **2022**, *140*, 108982. [[CrossRef](#)]
11. Yue, H.; Liu, Y.; Li, Y.; Lu, Y. Eco-Environmental Quality Assessment in China’s 35 Major Cities Based on Remote Sensing Ecological Index. *IEEE Access* **2019**, *7*, 51295–51311. [[CrossRef](#)]
12. Zhu, Q.; Guo, J.; Guo, X.; Chen, L.; Han, Y.; Liu, S. Relationship between ecological quality and ecosystem services in a red soil hilly watershed in southern China. *Ecol. Indic.* **2021**, *121*, 107119. [[CrossRef](#)]
13. Zhu, D.; Chen, T.; Wang, Z.; Niu, R. Detecting ecological spatial-temporal changes by Remote Sensing Ecological Index with local adaptability. *J. Environ. Manage.* **2021**, *299*, 113655. [[CrossRef](#)] [[PubMed](#)]
14. Zhang, X.; Kong, Y.; Ding, X. How High-Quality Urbanization Affects Utilization Efficiency of Agricultural Water Resources in the Yellow River Basin under Double Control Action? *Sustainability* **2020**, *12*, 2869. [[CrossRef](#)]
15. Wang, C.; Wang, L.; Zhan, J.; Liu, W.; Teng, Y.; Chu, X.; Wang, H. Spatial heterogeneity of urbanization impacts on ecosystem services in the urban agglomerations along the Yellow River, China. *Ecol. Eng.* **2022**, *182*, 106717. [[CrossRef](#)]
16. Li, J.; Sun, W.; Li, M.; Meng, L. Coupling coordination degree of production, living and ecological spaces and its influencing factors in the Yellow River Basin. *J. Clean. Prod.* **2021**, *298*, 126803. [[CrossRef](#)]
17. Ren, Y.; Bai, Y.; Liu, Y.; Wang, J.; Zhang, F.; Wang, Z. Conflict or Coordination? Analysis of Spatio-Temporal Coupling Relationship between Urbanization and Eco-Efficiency: A Case Study of Urban Agglomerations in the Yellow River Basin, China. *Land* **2022**, *11*, 882. [[CrossRef](#)]
18. Guo, P.; Zhang, F.; Wang, H. The response of ecosystem service value to land use change in the middle and lower Yellow River: A case study of the Henan section. *Ecol. Indic.* **2022**, *140*, 109019. [[CrossRef](#)]
19. Cui, R.; Han, J.; Hu, Z. Assessment of Spatial Temporal Changes of Ecological Environment Quality: A Case Study in Huaibei City, China. *Land* **2022**, *11*, 944. [[CrossRef](#)]
20. Wu, S.; Zhou, S.; Chen, D.; Wei, Z.; Dai, L.; Li, X. Determining the contributions of urbanisation and climate change to NPP variations over the last decade in the Yangtze River Delta, China. *Sci. Total Environ.* **2014**, *472*, 397–406. [[CrossRef](#)]
21. Wang, C.; Jiang, Q.; Shao, Y.; Sun, S.; Xiao, L.; Guo, J. Ecological environment assessment based on land use simulation: A case study in the Heihe River Basin. *Sci. Total Environ.* **2019**, *697*, 133928. [[CrossRef](#)] [[PubMed](#)]
22. Zhao, W.; Yan, T.; Ding, X.; Peng, S.; Chen, H.; Fu, Y.; Zhou, Z. Response of ecological quality to the evolution of land use structure in Taiyuan during 2003 to 2018. *Alex. Eng. J.* **2021**, *60*, 1777–1785. [[CrossRef](#)]
23. Xu, H. A remote sensing urban ecological index and its application. *Acta Ecol. Sin.* **2013**, *33*, 7853–7862.
24. Hu, X.; Xu, H. A new remote sensing index for assessing the spatial heterogeneity in urban ecological quality: A case from Fuzhou City, China. *Ecol. Indic.* **2018**, *89*, 11–21. [[CrossRef](#)]
25. Zheng, Z.; Wu, Z.; Chen, Y.; Guo, C.; Marinello, F. Instability of remote sensing based ecological index (RSEI) and its improvement for time series analysis. *Sci. Total Environ.* **2022**, *814*, 152595. [[CrossRef](#)]
26. Xu, H.; Wang, Y.; Guan, H.; Shi, T.; Hu, X. Detecting Ecological Changes with a Remote Sensing Based Ecological Index (RSEI) Produced Time Series and Change Vector Analysis. *Remote Sens.* **2019**, *11*, 2345. [[CrossRef](#)]
27. Liao, W.; Jiang, W. Evaluation of the Spatiotemporal Variations in the Eco-environmental Quality in China Based on the Remote Sensing Ecological Index. *Remote Sens.* **2020**, *12*, 2462. [[CrossRef](#)]
28. Xia, Q.; Chen, Y.; Zhang, X.; Ding, J. Spatiotemporal Changes in Ecological Quality and Its Associated Driving Factors in Central Asia. *Remote Sens.* **2022**, *14*, 3500. [[CrossRef](#)]

29. Ji, J.; Wang, S.; Zhou, Y.; Liu, W.; Wang, L. Studying the Eco-Environmental Quality Variations of Jing-Jin-Ji Urban Agglomeration and Its Driving Factors in Different Ecosystem Service Regions From 2001 to 2015. *IEEE Access* **2020**, *8*, 154940–154952. [[CrossRef](#)]
30. Huang, H.; Chen, W.; Zhang, Y.; Qiao, L.; Du, Y. Analysis of ecological quality in Lhasa Metropolitan Area during 1990–2017 based on remote sensing and Google Earth Engine platform. *J. Geogr. Sci.* **2021**, *31*, 265–280. [[CrossRef](#)]
31. Hang, X.; Li, Y.; Luo, X.; Xu, M.; Han, X. Assessing the Ecological Quality of Nanjing during Its Urbanization Process by Using Satellite, Meteorological, and Socioeconomic Data. *J. Meteorol. Res.* **2020**, *34*, 280–293. [[CrossRef](#)]
32. Gao, W.; Zhang, S.; Rao, X.; Lin, X.; Li, R. Landsat TM/OLI-Based Ecological and Environmental Quality Survey of Yellow River Basin, Inner Mongolia Section. *Remote Sens.* **2021**, *13*, 4477. [[CrossRef](#)]
33. Boori, M.S.; Choudhary, K.; Paringer, R.; Kupriyanov, A. Spatiotemporal ecological vulnerability analysis with statistical correlation based on satellite remote sensing in Samara, Russia. *J. Environ. Manag.* **2021**, *285*, 112138. [[CrossRef](#)] [[PubMed](#)]
34. Yuan, B.; Fu, L.; Zou, Y.; Zhang, S.; Chen, X.; Li, F.; Deng, Z.; Xie, Y. Spatiotemporal change detection of ecological quality and the associated affecting factors in Dongting Lake Basin, based on RSEI. *J. Clean. Prod.* **2021**, *302*, 126995. [[CrossRef](#)]
35. Liu, C.; Yang, M.; Hou, Y.; Zhao, Y.; Xue, X. Spatiotemporal evolution of island ecological quality under different urban densities: A comparative analysis of Xiamen and Kinmen Islands, southeast China. *Ecol. Indic.* **2021**, *124*, 107438. [[CrossRef](#)]
36. Wen, X.; Ming, Y.; Gao, Y.; Hu, X. Dynamic Monitoring and Analysis of Ecological Quality of Pingtan Comprehensive Experimental Zone, a New Type of Sea Island City, Based on RSEI. *Sustainability* **2020**, *12*, 21. [[CrossRef](#)]
37. Nie, X.; Hu, Z.; Zhu, Q.; Ruan, M. Research on Temporal and Spatial Resolution and the Driving Forces of Ecological Environment Quality in Coal Mining Areas Considering Topographic Correction. *Remote Sens.* **2021**, *13*, 2815. [[CrossRef](#)]
38. Jing, Y.; Zhang, F.; He, Y.; Kung, H.-T.; Johnson, V.C.; Arikena, M. Assessment of spatial and temporal variation of ecological environment quality in Ebinur Lake Wetland National Nature Reserve, Xinjiang, China. *Ecol. Indic.* **2020**, *110*, 105874. [[CrossRef](#)]
39. Ji, J.; Tang, Z.; Zhang, W.; Liu, W.; Jin, B.; Xi, X.; Wang, F.; Zhang, R.; Guo, B.; Xu, Z.; et al. Spatiotemporal and Multiscale Analysis of the Coupling Coordination Degree between Economic Development Equality and Eco-Environmental Quality in China from 2001 to 2020. *Remote Sens.* **2022**, *14*, 737. [[CrossRef](#)]
40. Shan, W.; Jin, X.; Ren, J.; Wang, Y.; Xu, Z.; Fan, Y.; Gu, Z.; Hong, C.; Lin, J.; Zhou, Y. Ecological environment quality assessment based on remote sensing data for land consolidation. *J. Clean. Prod.* **2019**, *239*, 118126. [[CrossRef](#)]
41. Xu, H.; Wang, M.; Shi, T.; Guan, H.; Fang, C.; Lin, Z. Prediction of ecological effects of potential population and impervious surface increases using a remote sensing based ecological index (RSEI). *Ecol. Indic.* **2018**, *93*, 730–740. [[CrossRef](#)]
42. Sun, C.; Li, X.; Zhang, W.; Li, X. Evolution of Ecological Security in the Tableland Region of the Chinese Loess Plateau Using a Remote-Sensing-Based Index. *Sustainability* **2020**, *12*, 3489. [[CrossRef](#)]
43. Ji, J.; Wang, S.; Zhou, Y.; Liu, W.; Wang, L. Spatiotemporal Change and Landscape Pattern Variation of Eco-Environmental Quality in Jing-Jin-Ji Urban Agglomeration From 2001 to 2015. *IEEE Access* **2020**, *8*, 125534–125548. [[CrossRef](#)]
44. Yan, Y.; Zhuang, Q.; Zan, C.; Ren, J.; Yang, L.; Wen, Y.; Zeng, S.; Zhang, Q.; Kong, L. Using the Google Earth Engine to rapidly monitor impacts of geohazards on ecological quality in highly susceptible areas. *Ecol. Indic.* **2021**, *132*, 108258. [[CrossRef](#)]
45. Hou, Y.; Chen, Y.; Ding, J.; Li, Z.; Li, Y.; Sun, F. Ecological Impacts of Land Use Change in the Arid Tarim River Basin of China. *Remote Sens.* **2022**, *14*, 1894. [[CrossRef](#)]
46. Ferraz, S.F.D.B.; Vettorazzi, C.A.; Theobald, D.M. Using indicators of deforestation and land-use dynamics to support conservation strategies: A case study of central Rondônia, Brazil. *For. Ecol. Manag.* **2009**, *257*, 1586–1595. [[CrossRef](#)]
47. Wang, J.; Li, X.; Christakos, G.; Liao, Y.; Zhang, T.; Gu, X.; Zheng, X.-Y. Geographical Detectors-Based Health Risk Assessment and its Application in the Neural Tube Defects Study of the Heshun Region, China. *Int. J. Geogr. Inf. Sci.* **2010**, *24*, 107–127. [[CrossRef](#)]
48. Cai, M. Land for welfare in China. *Land Use Policy* **2016**, *55*, 1–12. [[CrossRef](#)]
49. Shen, X.; Wang, L.; Wu, C.; Lv, T.; Lu, Z.; Luo, W.; Li, G. Local interests or centralized targets? How China’s local government implements the farmland policy of Requisition–Compensation Balance. *Land Use Policy* **2017**, *67*, 716–724. [[CrossRef](#)]
50. Liu, Y.; Fang, F.; Li, Y. Key issues of land use in China and implications for policy making. *Land Use Policy* **2014**, *40*, 6–12. [[CrossRef](#)]
51. Chien, S. Local farmland loss and preservation in China—A perspective of quota territorialization. *Land Use Policy* **2015**, *49*, 65–74. [[CrossRef](#)]
52. Liu, C.; Zhang, X.; Wang, T.; Chen, G.; Zhu, K.; Wang, Q.; Wang, J. Detection of vegetation coverage changes in the Yellow River Basin from 2003 to 2020. *Ecol. Indic.* **2022**, *138*, 108818. [[CrossRef](#)]
53. Guo, B.; Niu, Y.; Mantravadi, V.S.; Zhang, L.; Liu, G. The variation of rainfall runoff after vegetation restoration in upper reaches of the Yellow River by the remote sensing technology. *Environ. Sci. Pollut. Res. Int.* **2021**, *28*, 50707–50717. [[CrossRef](#)] [[PubMed](#)]
54. Xu, G.; Zhang, J.; Li, P.; Li, Z.; Lu, K.; Wang, X.; Wang, F.; Cheng, Y.; Wang, B. Vegetation restoration projects and their influence on runoff and sediment in China. *Ecol. Indic.* **2018**, *95*, 233–241. [[CrossRef](#)]
55. Yu, Z.; Zhang, J.; Yang, G. How to build a heat network to alleviate surface heat island effect? *Sustain. Cities Soc.* **2021**, *74*, 103135. [[CrossRef](#)]
56. Chun, B.; Guldmann, J.-M. Impact of greening on the urban heat island: Seasonal variations and mitigation strategies. *Comput. Environ. Urban Syst.* **2018**, *71*, 165–176. [[CrossRef](#)]
57. Salata, S.; Grillenzoni, C. A spatial evaluation of multifunctional Ecosystem Service networks using Principal Component Analysis: A case of study in Turin, Italy. *Ecol. Indic.* **2021**, *127*, 107758. [[CrossRef](#)]

58. Liang, C.; Zeng, J.; Zhang, R.-C.; Wang, Q.-W. Connecting urban area with rural hinterland: A stepwise ecological security network construction approach in the urban–rural fringe. *Ecol. Indic.* **2022**, *138*, 108794. [[CrossRef](#)]
59. Cui, L.; Wang, J.; Sun, L.; Lv, C. Construction and optimization of green space ecological networks in urban fringe areas: A case study with the urban fringe area of Tongzhou district in Beijing. *J. Clean. Prod.* **2020**, *276*, 124266. [[CrossRef](#)]
60. Dadashpoor, H.; Azizi, P.; Moghadasi, M. Land use change, urbanization, and change in landscape pattern in a metropolitan area. *Sci. Total Environ.* **2019**, *655*, 707–719. [[CrossRef](#)] [[PubMed](#)]
61. Deng, J.; Wang, K.; Hong, Y.; Qi, J. Spatio-temporal dynamics and evolution of land use change and landscape pattern in response to rapid urbanization. *Landsc. Urban Plan.* **2009**, *92*, 187–198. [[CrossRef](#)]